JOURNAL OF MATERIALS SCIENCE **34** (1999) 551–555

Morphology and growth mechanism of silicon carbide chemical vapor deposited at low temperatures and normal atmosphere

Y. XU, L. CHENG, L. ZHANG, W. ZHOU
State Key Laboratory of Solidification Processing, Northwestern Polytechnical University, Xi'an, Shaanxi 710 072, People's Republic of China
E-mail: ydxu@nwpu.edu.cn

With the method of phenomenology, a supersaturation–condensation–fusion (SCF) mechanism is proposed to describe the growth of chemical vapor deposition silicon carbide under normal atmosphere. The structure has been characterized by scanning electron microscopy and transmission electron microscopy. Morphology characterization of deposited crystallites and silicon carbide aggregates have been explained in terms of SCF mechanism; Raman spectra analysis indicated that the major chemical bonds of deposit were Si–C and –C=C–. Auger spectra analysis revealed that there were Si, C, S, Cl, and O on the surface of the deposit.

1. Introduction

Chemical vapor deposition (CVD) and derived chemical vapor infiltration (CVI) techniques have been well developed and used to prepare silicon carbide (SiC) oxidation protection coating for carbon/carbon composites (C/C) and ceramic matrix composites [1–4]. Compared with reactions between liquids and solids, the reactions between the gaseous species in CVD are more complex and difficult to control because more median reactions are involved in the CVD process. As a result, a small variation in deposition conditions contributes to the significant differences in both the morphology and microstructure of the deposit. Usually, the properties of the deposit are mainly dependent on the microstructure characterization and morphology of the materials, which are strongly controlled by the growth behavior of the deposit.

Based on the single-layer theory, the typical CVD mechanism was developed, a mechanism usually described as follows [5, 6]: (1) transport of reactant species to the vicinity of the substrate; (2) diffusion of reactant species to the substrate surface; (3) adsorption of reactant species; (4) surface diffusion, dissociation, inclusion of coating atoms into the growing surface, and formation of by-product species; (5) de-absorption of by-product species; (6) diffusion of by-product species into the bulk gas; and (7) transport of by-product species away from the substrate (exhaust). This theory successfully explains the morphology of the thin film deposited high temperatures and low atmosphere pressure. However, it is difficult to interpret the aggregate morphology that appeared at low deposition temperature and high atmosphere pressure. In the typical deposition theory, the gaseous species was considered in the molecular state. In fact, the gaseous species was in an ionic state because of decomposition at high temperatures. The research on morphology deposit is usually based on the thermodynamic calculations of chemical reactions.

The purposes of the current article are to examine the chemical composition and microstructure of silicon carbide deposited at low temperatures and normal atmosphere pressure, and to investigate the growth mechanism of silicon carbide with the method of phenomenology.

2. Experimental procedure

2.1. Materials preparation

Silicon carbide examined in the current study was chemical vapor deposited at various temperatures ranging from 1000 to 1300 °C at a normal atmosphere. High-purity graphite film and T-300 carbon fiber were used as deposition substrates. Methyltrichlorosilane (CH_3SiCl_3 or MTS) was employed to deposit silicon carbide because it contains the same number of silicon and carbon atoms in one MTS molecule and thus can easily prepare stoichiometric silicon carbon [7–10]. MTS was maintained at a constant temperature and carried to the reaction chamber by bubbling hydrogen gas. In each run, the substrates were pre-cleaned and preheated above the deposition temperature in hydrogen for 30 min. The typical condition now being used for deposition is a hydrogen-to-MTS mole ratio of 10. Argon was used as dilute gas to slow the reaction rate. The details of the deposition apparatus and conditions have been described elsewhere [11, 12].

2.2. Observation of the deposit

X-ray diffraction (XRD) measurements were made with a Rigaku D/Max-B diffractometer unit using Ni-filtered CuK_α radiation at a scanning rate of $0.5^\circ \cdot \text{sec}^{-1}$

and scanning from 20° to 80° of 2θ. The surface morphology and cross-sectional microstructure of the deposited films were observed using scanning electronic microscopy (SEM, Model Jeol 840). The surface chemical composition and chemical bonds were examined with scanning multiple Auger Probe (Perkin-Elmers) and Raman spectra (U1000 Laser Raman Microprobe). Transmission electron microscopy (TEM, Jeol 2000 fx) was used to characterize the crystal structure and bulk microstructure of the deposits. TEM samples were cut to a thickness of 300 μm using a low special diamond saw, mechanically thinned to 75 μm, and then dimpled to a center using Ar^+ ions at an incident angle of 15°. The specimens were examined in an operated at 200 kV.

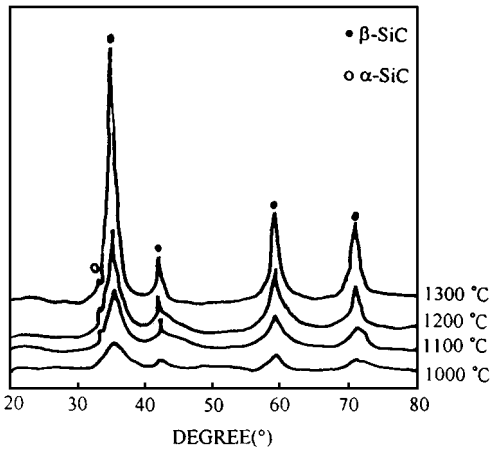

Figure 1 XRD patterns of the deposit at various temperatures.

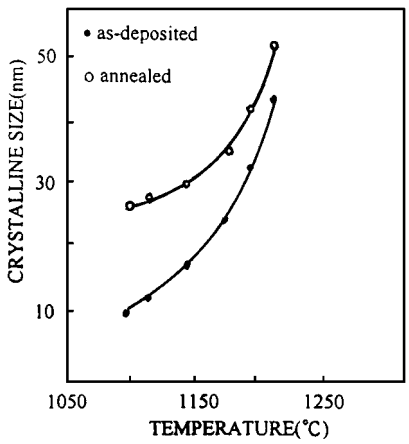

Figure 2 Relationship between crystalline size versus deposition temperature.

3. Results and discussion

3.1. The characterization of the deposit

XRD patterns of the deposit at various temperatures are shown in Fig. 1. Detailed analysis of the X-ray results indicated that the deposits are pure silicon carbide composed mainly of cubic (3C) type β-SiC with a small amount of 4H type α-SiC. It is clear that the diffraction angles of 35.6°, 41.3°, 60.1°, 72.1°, and 75.5° correspond to β-SiC with cubic crystal structure and the diffraction angle of 33.7° corresponds to α-SiC with the hexagonal crystal structure [13]. As deposition temperatures decrease, the deposit became poorly crystallized because the diffraction angles became broader. At the deposition temperature of 1000 °C, the deposit was in a quasi-amorphous state. According to the breadth of diffraction peaks, the crystallite sizes of silicon carbide were calculated from the Scherrer equation [14],

$$D = 0.89\lambda/\beta\,\mathrm{COS}(\theta)$$

where λ is the wavelength of characteristic X-rays, θ is the Bragg angle, and β is the calibrated width of the half-height of diffraction peaks.

The relationship between crystalline size versus deposition temperature is shown in Fig. 2. With the deposition temperature increased from 1000 to 1300 °C, the crystallite size increased from 10 to 45 nm. The dependence of crystallite size on deposition temperature was attributed to the mobilities at different temperatures, that is, high deposition temperatures led to high mobility of individual atoms over the crystalline surface and resulted in the formation of large crystallite size and small lattice distortion, whereas low surface mobility of atoms led to small crystallite size at lower deposition temperatures.

The surface chemical composition of silicon carbide was analyzed by Auger probe, and the results are shown in Fig. 3. Besides silicon and carbon, the elements S, Cl, and O were also found on the deposited silicon carbide surface. After the sample was sputtered for 5 min, S and Cl were not detected, and the amount of O was obviously decreased. O disappeared completely after

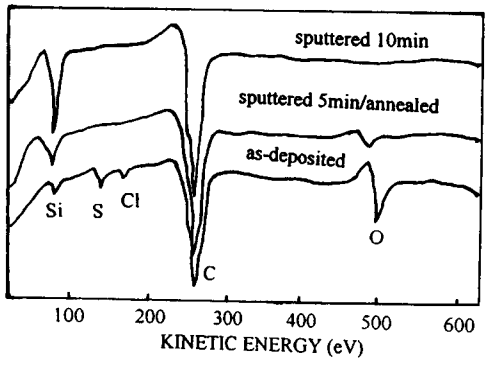

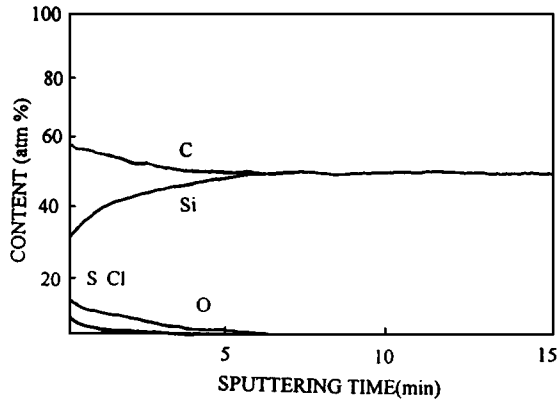

Figure 3 Auger spectra of surface chemical composition of silicon carbide.

the sample was sputtered for another 5 min. The sputter rate was 0.02 nm · sec^{-1}. It is clear that S, Cl, and O were only located in a very thin layer ($\sim$24 nm) on the surface of the silicon carbide. Furthermore, both S and Cl were absorbed on the surface and derived from the reaction gaseous species of MTS. O existed in the form of silica and was from the residual O_2 and H_2O in the reactant system. Experiments also indicated that even only a very small amount of O_2 could result in the formation of silica.

3.2. Morphology of CVD SiC on the graphite substrate

The morphology of the CVD SiC is very sensitive to the deposition temperature, which is shown in Fig. 4. At the deposition temperature of 1000 °C, the deposit is composed of a large number of spherical particles with a cloud-cluster shape. Among these particles, aggregation and fusion are also observed. As discussed in the section above on XRD results, it is easy to determine that each particle is an aggregate consisting of a large number of nanometer SiC crystallites rather than one SiC single crystallite. Morever, there are many pores among the aggregates in the cross-section resulting from the incomplete fusion of the particles. As the deposition temperature was increased to 1100 °C, the particles became larger than those deposited at 1000 °C. From the cross-section of the microstructure, it is observed that the deposited film became very dense. At the deposition temperature of 1200 °C, the size of particles was decreased, and no pores existed in the deposited film. It should be noted that many fine sub-particles were observed on the surface of based particles. When the deposition temperature was increased to 1300 °C, the morphology of the deposit became cauliflower-like.

With regards to chemical reaction kinetics, CVD involves two processes, i.e., gaseous species mass transport and chemical reaction [12]. At low temperatures, chemical reaction is the limited process, but at relatively high temperatures, the limited process is shifted to gaseous species mass transport. At a deposition temperature of 1000 °C, the chemical reaction proceeds very slowly. As the deposition proceeds, the supersaturation of reactant species is increased because the partial pressure of reactant species increases within the boundary layer of graphite substrate. According to the gas dynamics [15], the condensation of the vapor would occur if the supersaturation degree reaches the critical values. The condensation in the boundary layer would lead to the formation of liquid droplets composed of Si, C, Cl, and H.

According to the Gibbs–Thomson relation [16], the correspondence between crystal size (B) (or aggregate size) of droplets and supersaturation ($\Delta\mu$) can be expressed by:

$$B \propto 1/\ln(\Delta\mu)$$

The increase of deposition temperature results in a rapid chemical reaction rate, and the decrease of supersaturation, in turn, leads to an increase of crystal size of condensed liquid droplets. Consequently, the size of SiC aggregates also increased. It should be noted that the temperature became higher near the direction of the deposition substrate. Accordingly, the contents of both Cl and H were decreased and eventually became stoichiometric SiC aggregates as liquid droplets moved to the surface of the substrate in the boundary layer, and the temperature increased. Raman spectra results revealed that the main chemical bonds are Si–C and –C=C– bonded on the surface of deposit (Fig. 5).

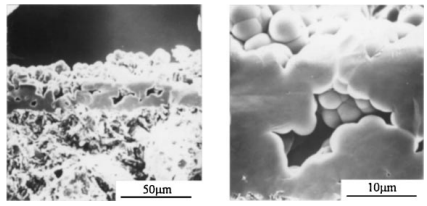

(a) Deposition temperature 1000 °C

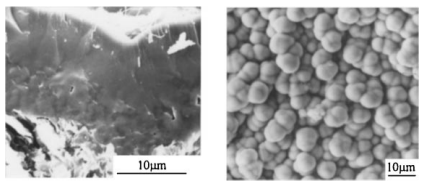

(b) Deposition temperature 1100 °C

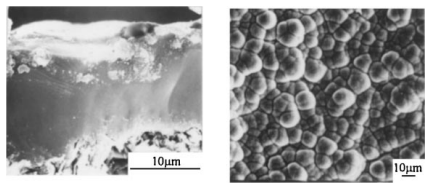

(c) Deposition temperature 1200 °C

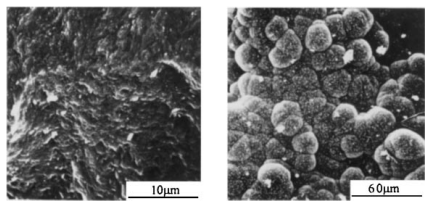

(d) Deposition temperature 1300 °C

Figure 4 Microstructure of CVD SiC on the graphite substrate.

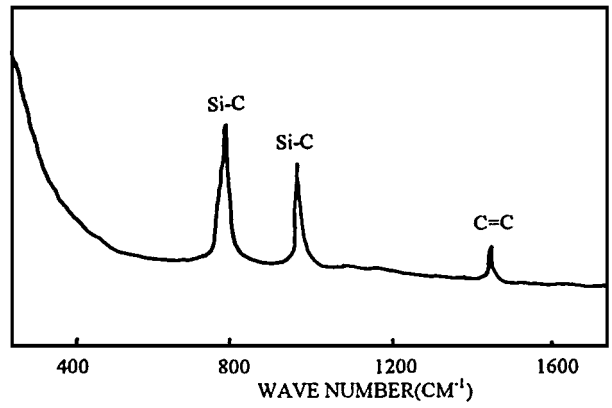

Figure 5 Raman spectra of silicon carbide surface.

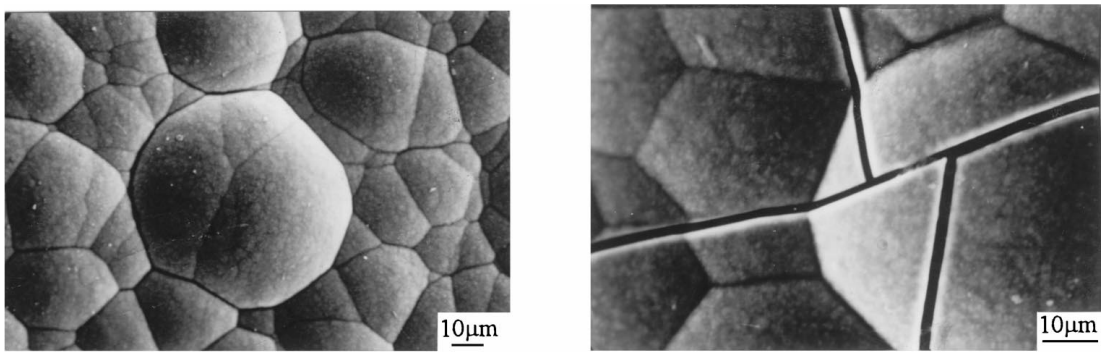

Figure 6 The typical equiaxed morphology of CVD SiC on the graphite substrate.

At high deposition temperatures (1000 °C), the substance diffusion is very difficult because of the high active energy of surface diffusion. Consequently, the aggregates maintain the as-formed spherical morphology. Furthermore, it is very difficult for the as-formed liquid droplets to fuse together, and as a result, there are many pores within the deposited SiC film. As the deposition temperature increases, the active energy of surface diffusion is reduced. The surface diffusion led to the fusion among the aggregates and crystal growth of SiC crystallites. As a result, the size of both aggregates and SiC crystallites increased, and the porosity of the deposited film also decreased.

The presence of liquid droplets could be confirmed by the microstructure shown in Fig. 6. With regards to solidification theory, the typical and stable characterization of solidified morphology from liquid is an equiaxed structure in hexagonal form. The microcracks in the texture of the deposit are attributed to the difference of the thermal expansion coefficient. At the deposition temperature of 1300 °C, the chemical reaction proceeds very rapidly and the activities of atoms are also increased further. Therefore, the liquid droplets fused completely together, and no pores were present in the deposited film. Furthermore, the crystal size of SiC also increased and can be observed in SEM micrographs. The aggregates are observed in cauliflower-like form.

3.3. Morphology of CVD SiC on T-300 carbon fiber substrate

At the deposition temperature of 1100 °C, the morphologies are as shown in Fig. 7 and the aggregates are in the state of planets perpendicular to the axial of the carbon fibers. Obviously, the morphologies are significantly different than those on the graphite substrate.

In the TEM micrographs (Fig. 8), the microstructure can be classified into three groups: (1) a very thin layer of fine crystallites with isotropy near the carbon fiber; (2) the fish-scale-like layer with large crystallites; and (3) the laminated layer with larger SiC crystallites, which is located outside of the coated fiber.

Further observation demonstrated that there is another substructure within both fish-plane layer and the plane layer in the form of deformed spheres. There are a large number of nano-crystals and pores among the spheres.

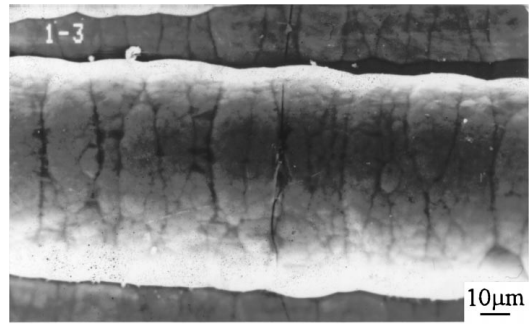

Figure 7 SEM micrograph of the microstructure of CVD SiC on the carbon fiber.

The morphology difference of the deposit between the results on the graphite and carbon fiber is attributed to the deformation of the droplets. On the graphite substrate, the droplets can be easily absorbed on the substrate without deformation, so the aggregates maintained the as-formed form. The most stable form of droplets is in the hexagonal state, which is demonstrated in Fig. 6. As far as carbon fiber with a cylindrical form, the aggregates should be deformed to suit the substrate form. Subsequently, the plane structure is observed.

The supersaturation–condensation–fusion (SCF) deposition mechanism is proposed as follows. The deposition is defined in two stages: the first stage includes the initial part in which the deposition obeys the typical CVD mechanism and is constrained in a very thin layer. As the deposition proceeds, the supersaturation of the chemical reaction system is increased constantly, which results in the formation of liquid droplets. It should be noted that the droplets consisted of the elements Si, C, H, and Cl and could be deformed. The contents of H and Cl are decreased with the moving to the surface of the substrate, and stoichiometric silicon carbide ($Si : C = 1 : 1$) is eventually obtained. Meanwhile, the liquid droplets fused to each other to form solid film. As the deposition temperature increased, the sizes of both aggregates and SiC crystallites also increased. The morphology of the deposited SiC film is shifted from cloud-like with a smooth surface to a cauliflower-like surface.

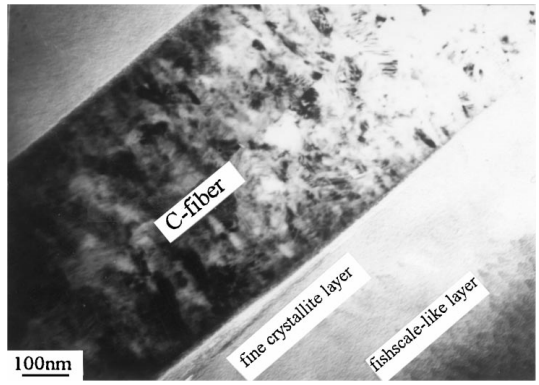

(a) Fishscale layer on C-fiber

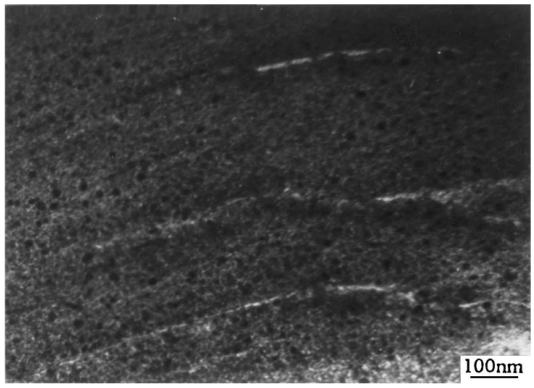

(b) Laminated layer

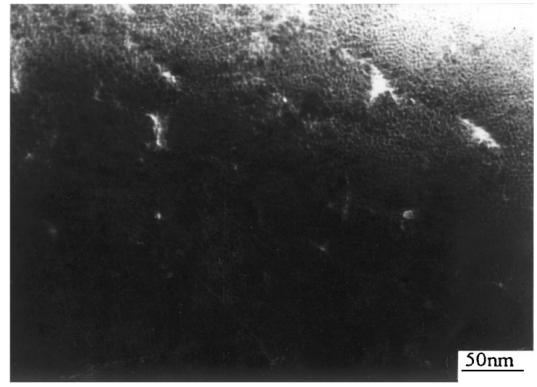

(c) Sub-structure in the deposit

Figure 8 TEM micrographs of the microstructure of CVD SiC on the carbon fiber.

4. Conclusions

With the method of phenomenology, an SCF mechanism is proposed to describe the growth of CVD silicon carbide under a normal atmosphere. The structure has been characterized by SEM and TEM. When the deposition temperature increased from 1000 to 1300 °C, the crystallite size increased from 10 to 45 nm. Aggregate structures have been observed and explained in terms of SCF mechanism. The supersaturation of the chemical reaction system results in the formation of liquid droplets containing Si, C, H, and Cl. The contents of H and Cl are decreased with the moving to the surface of the substrate, and stoichiometric silicon carbide is eventually obtained. Raman spectra analysis indicated that the major chemical bonds of the deposit were Si–C and –C=C–. Auger spectra analysis revealed that there were Si, C, S, Cl, and O on the surface of the deposit.

Acknowledgements

The authors wish to thank the National Natural Scientific Foundation of China, the Chinese Aeronautics Foundation, and the National Defense Foundation of China for the financial support.

References

1. J. M. JAMET and P. J. LMICQ, in "High Temperature Ceramics Matrix Composites," edited by R. Naslain (Bordeaux: Woodhead; 1993) p. 735.
2. J. K. STRIFE and J. E. SHECHAN, *Am. Ceram. Soc. Bull.* **67** (1988) 367.
3. R. NASLAIN, in "Ceramic Matrix Composites," edited by R. Warren (London and New York: Champan & Hall, 1992) p. 199.
4. D. P. STINTON, T. M. BESMANN and R. A. LOWDEN, *Am. Ceram. Soc. Bull.* **67** (1988) 350.
5. T. M. BESMANN, R. A. LOWDEN and D. P. STINTION, in "High Temperature Ceramics Matrix Composites," edited by R. Naslain (Bordeaux: Woodhead, 1993) p. 215.
6. A. G. SULEYMAN, in "Proceedings of the 11th International Conference on Chemical Vapor Deposition," edited by K. E. Spear (American Electrochemical Society, Pennington, New Jersey, 1990) p. 1.
7. D. P. STINTON, W. J. LACKEY, R. J. LAUF and T. M. BESMANN, *Ceram. Eng. Sci. Proc.* **5** (1984) 668.
8. K. MINATO and K. FUKUDA, *J. Mater. Sci.* **23** (1988) 699.
9. D. LESPIAUX, F. LANGLASIS and R. NASLAIN, *ibid.* **30** (1995) 1550.
10. W. J. LACKEY, J. A. HANIGOFSKY, G. B. FREEMAN, R. D. HARDIN and A. PRASAD, *J. Am. Ceram. Soc.* **78** (1995) 1564.
11. D. P. STINTON, A. J. CAPUTO and R. A. LOWDEN, *Am. Ceram. Soc. Bull.* **65** (1986) 347.
12. T. M. BESMANN, B. W. SHELDON, R. A. LOWDEN and D. P. STINTON, *Science* **235** (1991) 1104.
13. F. SIBIEUDE and G. BENEZECH, *J. Mater. Sci.* **22** (1988) 1623.
14. C. W. ZHU, G. Y. ZHAO, V. REVANKAR and V. HLAVACEK, *ibid.* **28** (1993) 659.
15. H. W. EMMONS, "Fundamentals of Gas Dynamics (Section F)" (Princeton, Princeton University Press, 1958) p. 3.
16. E. J. GIVARGIAOV, "Current Topics in Materials Science" (New York: North-Holland, 1978) p. 91.

Received 10 March
and accepted 14 July 1998